JOURNAL OF GUIDANCE, CONTROL, AND DYNAMICS
Vol. 25, No. 2, March–April 2002

Analysis of the Two-Degree-of-Freedom Wing Rock in Advanced Aircraft

Tiauw Hiong Go and Rudrapatna V. Ramnath
Massachusetts Institute of Technology, Cambridge, Massachusetts 02139

The dynamics of wing rock on rigid aircraft having two rotational degrees of freedom are analyzed. Nonlinear mathematical models of the aircraft are developed for the purpose of the analysis. The aerodynamic expressions contained in the models are built by fitting the appropriate aerodynamic data into the model. The nonlinear dynamics are analyzed using a technique combining the multiple time scales method, center manifold reduction principle, and bifurcation theory. Analytical solutions are developed in parametric forms showing a separation of the fast and slow dynamics. Such solutions have an advantage over numerical solutions in that the important parameters and their effects on wing rock characteristics, such as amplitude and frequency, are easily seen in explicit functional relationships. An excellent agreement between the analytical results and the numerical simulations is demonstrated.

Nomenclature

b	=	wing span
C_l	=	coefficient of rolling moment
C_m	=	coefficient of pitching moment
c	=	airfoil chord length
c_D	=	drag coefficient
c_L	=	lift coefficient
$\mathrm{d}D$	=	incremental drag force
$\mathrm{d}L$	=	incremental lift force
I_{ii}	=	moment of inertia about i axis
I_{ij}	=	product of inertia
$\boldsymbol{i}_{()}$	=	unit vector along the axis indicated in subscript
L_{p_0}	=	rolling moment due to roll rate
$L_{\dot{\beta}_0}$	=	rolling moment due to rate of sideslip
p	=	roll rate about X_b axis
q	=	pitch rate about Y_b axis
$\Re(\cdot)$	=	real part of the complex number in parentheses
r	=	yaw rate about Z_b axis
S	=	wing area
T	=	kinetic energy
t	=	time
V	=	airspeed
$X_bY_bZ_b$	=	right-handed Cartesian body-fixed axis system
$X_0Y_0Z_0$	=	right-handed Cartesian stability axis system
y	=	coordinate along Y_b axis
α	=	deviation of angle of attack from α_0
α_e	=	effective angle of attack
α_0	=	nominal angle of attack
β	=	angle of sideslip
ϵ	=	small parameter
θ	=	pitch angle
$\tilde{\mu}$	=	roll damping parameter, $\epsilon\mu$
$\tilde{\nu}$	=	pitch damping parameter, $\epsilon\nu$
ρ	=	air density
τ_i	=	time scales
ϕ	=	roll angle
$\boldsymbol{\omega}$	=	inertial angular velocity
∇_x	=	Jacobian of vector $\boldsymbol{x}$
$(\dot{\cdot})$	=	$\mathrm{d}/\mathrm{d}t(\cdot)$

Tiauw Hiong Go received his engineer's degree in Mechanical Engineering from Institut Teknologi Bandung, Indonesia in 1990, and his Master's and Sc.D. degrees in aeronautics and astronautics from Massachusetts Institute of Technology (MIT) in 1994 and 1999, respectively. His research interests include dynamics and control of aircraft and spacecraft, simulation, and human factors. Since 1999, he has been a postdoctoral associate at MIT, working in conjunction with the U.S. Department of Transportation Volpe Center on flight simulator fidelity requirements for pilot training and evaluation. He is currently a member of the AIAA Modeling and Simulation Technologies Committee.

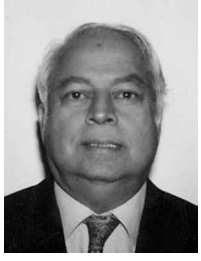

Rudrapatna V. Ramnath earned his B.E. (Electrical Engineering) degree from Bangalore University, India in 1959 and M.Sc. in Electrical Engineering from Cransfield Institute of Technology, U.K. in 1963, specializing in flight control. He then received the M.S.E., M.A., and Ph.D. degrees in Aerospace and Mechanical Engineering from Princeton University in 1965, 1966, and 1968, respectively. His experience includes work as Division Leader at Draper Laboratory and Consulting Engineer at Raytheon. As Adjunct Professor and Senior Lecturer at Massachusetts Institute of Technology, since 1979 he has taught topics such as aircraft and spacecraft dynamics and control, multiple time scale systems, nonlinear control, and related subjects in which he continues his research.

Received 11 May 2000; revision received 1 May 2001; accepted for publication 18 July 2001.

I. Introduction

MOST modern fighter aircraft are required to have high-performance capabilities for enhanced air superiority. Such requirements necessitate an aircraft to operate in nonlinear flight regimes in which the dynamics are very complex. An important manifestation of the effect of nonlinearities is the phenomenon of wing rock, which limits the potential maneuver performance of the aircraft and could even lead to catastrophic consequences. It usually occurs at moderate to high angles of attack and involves sustained lateral oscillations dominated by roll motion at a constant amplitude and definite frequency. The degree of severity of wing rock is determined mainly by the amplitude of the motion and to a lesser extent by the period of the oscillation.

Several kinds of wing rock problems have been treated in the literature. In general, wing rock manifests as a limit-cycle-type of oscillation. The case most extensively treated is wing rock with roll as the only one rotational degree of freedom.[1–7] Both numerical and analytical techniques have been used in the past to attack the problem. It has been found that for this specific case the onset of wing rock is determined by the loss of the dynamic roll damping derivative and that its amplitude is mainly influenced by the nonlinearity in the derivative of the roll moment coefficient with respect to roll rate. Investigations of wing rock on aircraft having multiple rotational degrees of freedom have also been initiated. Because of the complexity of the problem, most work in this area is numerical in nature,[8–12] and therefore, the results are only valid for specific cases.

This paper presents a part of the results obtained in Ref. 13, in which wing rock dynamics of a rigid aircraft having two rotational degrees of freedom in roll and pitch are discussed. This two-degree-of-freedom assumption is good for an aircraft with negligible yaw dynamics during the motion of interest. An analytical approach using the multiple time scales (MTS) method[14,15] in conjunction with the center manifold reduction and bifurcation theory is used in the analysis to obtain an asymptotic solution of the problem. The interdependence of the pitch degree of freedom and the wing rock motion is shown explicitly in this investigation. This approach offers considerable advantages over the common numerical approaches in that it enables us to gain insight into the system dynamics and to identify the important parameters that influence the overall motion.

II. Equations of Motion

Two axis systems are used in deriving the equations of motion. The first set of axes $(X_b Y_b Z_b)$ is the body-fixed axis system, which is fixed to the aircraft body and has its origin at the center of mass of the aircraft. The X_b axis points toward the nose of the aircraft, the Z_b axis is perpendicular to X_b in the aircraft vertical plane, and the Y_b axis completes the right-handed axis system. The X_b–Z_b plane is the vertical symmetry plane of the aircraft. The second set of axes $(X_0 Y_0 Z_0)$ is referred to as the stability axis system. Its origin is at the center of mass of the aircraft, and the orientation of the axes describes the nominal or unperturbed attitude of the aircraft. The X_0 axis is oriented toward the nominal nose direction of the aircraft, the Z_0 axis is in the nominal vertical plane of the aircraft pointing down and perpendicular to the X_0 axis, and the Y_0 axis completes the right-handed axis system. In the nominal flight condition, these two axis systems coincide with each other.

The expression for the aircraft angular rate in the body-fixed axes can be found by noting that the aircraft can be brought from its nominal position to the perturbed one by using two consecutive rotations, first in pitch and then in roll (Fig. 1). Hence,

$$\boldsymbol{\omega} = p\boldsymbol{i}_{x_b} + q\boldsymbol{i}_{y_b} + r\boldsymbol{i}_{z_b} = \dot{\theta}\boldsymbol{i}_{y_0} + \dot{\phi}\boldsymbol{i}_{x_b} \tag{1}$$

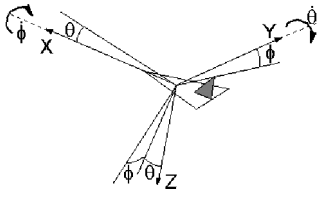

Fig. 1 Transform angles and rotations between the stability and body-fixed axis systems.

As per usual convention, p, q, and r are the roll rate, pitch rate, and yaw rate, respectively, of the aircraft; and ϕ and θ are the roll and pitch angular perturbations from the nominal position. Then by assuming that the perturbation angles are small, the following relations are obtained:

$$p = \dot{\phi}, \qquad q = \dot{\theta}\cos\phi \approx \dot{\theta}, \qquad r = -\dot{\theta}\sin\phi \approx -\phi\dot{\theta} \tag{2}$$

Note that r is not zero in this case. Its magnitude, however, is one order of magnitude smaller than p and q.

We further assume that the aircraft body is symmetric, so that the product of inertia $I_{xy} = I_{yz} = 0$. The rotational kinetic energy of the aircraft can then be expressed as follows:

$$T = \tfrac{1}{2}I_{xx}\dot{\phi}^2 + \tfrac{1}{2}I_{yy}\dot{\theta}^2 + \tfrac{1}{2}I_{zz}\phi^2\dot{\theta}^2 - I_{xz}\phi\dot{\phi}\dot{\theta} \tag{3}$$

where I_{xx}, I_{yy}, and I_{zz} are the moment of inertia of the aircraft about X_b, Y_b, and Z_b, respectively. By the substitution of this expression into Lagrange's equation,

$$\frac{\mathrm{d}}{\mathrm{d}t}\left(\frac{\partial T}{\partial \dot{\gamma}_i}\right) - \frac{\partial T}{\partial \gamma_i} = Q_i, \qquad i = 1, 2 \tag{4}$$

where $\gamma_1 = \phi$ and $\gamma_2 = \theta$, we get

$$\begin{aligned} I_{xx}\ddot{\phi} + I_{xz}\phi\ddot{\theta} + I_{xz}\dot{\phi}\dot{\theta} - I_{zz}\phi\dot{\theta}^2 &= Q_1 \\ \left(I_{yy} + I_{zz}\phi^2\right)\ddot{\theta} + I_{xz}\phi\ddot{\phi} + I_{xz}\dot{\phi}^2 + 2I_{zz}\phi\dot{\phi}\dot{\theta} &= Q_2 \end{aligned} \tag{5}$$

where the generalized force $Q_i = \delta W_i/\delta\gamma_i$, which is the variation of the work done δW_i due to the variation of the displacement $\delta\gamma_i$. The generalized forces are assumed to be solely due to the aerodynamic moments. The effect of gravity is neglected in the current analysis.

The aerodynamic moments acting on the aircraft are derived under the assumption that the flow is nearly incompressible and quasi steady. The purpose is not to get the exact aerodynamic formulation, but rather to find the appropriate mathematical expressions to represent the nonlinear aerodynamic moments to be used later in the analysis. The resulting moment expressions are expected to capture the parameters that have a significant impact on the system dynamics. Strip theory aerodynamics are utilized for this purpose. We assume that the aerodynamic forces are generated mainly by the wings. The aerodynamic forces on the fuselage and the tail are neglected. The fuselage does, however, have a significant presence and contributes to three-dimensional effects especially in the asymmetric flow case.

For each streamwise segment of the wing of width $\mathrm{d}y$, the incremental lift and drag forces are

$$\mathrm{d}L(y) = \bar{q}c(y)c_L(y)\,\mathrm{d}y, \qquad \mathrm{d}D(y) = \bar{q}c(y)c_D(y)\,\mathrm{d}y \tag{6}$$

where $\bar{q} = \frac{1}{2}\rho V^2$ is the dynamic pressure, $c(y)$ is the airfoil chord at location y along the Y_b axis, and $c_L(y)$ and $c_D(y)$ are the local lift and drag coefficients, respectively. The dependence of the local lift and drag coefficients $c_L(y)$ and $c_D(y)$ on the local effective angle of attack $\alpha_e(y)$ is represented by a cubic polynomial:

$$\begin{aligned} c_L &= c_{L_0} + c_{L_1}\alpha_e + c_{L_2}\alpha_e^2 + c_{L_3}\alpha_e^3 \\ c_D &= c_{D_0} + c_{D_1}\alpha_e + c_{D_2}\alpha_e^2 + c_{D_3}\alpha_e^3 \end{aligned} \tag{7}$$

For notational simplicity, the dependence of the coefficients and α on the spanwise location is not shown.

The effective angle-of-attack distribution along the wing span is influenced by the nominal angle of attack, the roll rate, the sideslip rate, the pitch rate, the rate of change of angle of attack and sideslip, and the deviation from the nominal angle of attack. The contribution of yaw rate r due to kinematic coupling is neglected here because its value is normally small for this two-degrees-of-freedom aircraft model. Because we only consider small deviations from the nominal

condition, the contributions of the named factors on the effective angle-of-attack distribution can be expressed using a linear relation

$$\alpha_e(y) = \alpha_1(y) + \frac{\partial \alpha_e(y)}{\partial p}p + \frac{\partial \alpha_e(y)}{\partial \beta}\beta + \frac{\partial \alpha_e(y)}{\partial \dot{\beta}}\dot{\beta} + \frac{\partial \alpha_e(y)}{\partial \alpha}\alpha + \frac{\partial \alpha_e(y)}{\partial q}q + \frac{\partial \alpha_e(y)}{\partial \dot{\alpha}}\dot{\alpha} \tag{8}$$

where $\alpha_1(y)$ indicates the contribution of the nominal angle of attack α_0. For simplicity, the spanwise angle-of-attack distribution due to roll rate, the sideslip rate, and the rate of change of sideslip is assumed to be antisymmetric, and the distribution due to the nominal angle of attack, the pitch rate, the rate of change of angle of attack, and the deviation from nominal angle of attack is assumed to be symmetric.

The substitution of Eq. (8) into Eq. (7) and the substitution of the resulting equation into Eq. (6) results in lengthy expressions involving the lift and drag forces on each segment of the wing and tail in terms of the variables p, β, $\dot{\beta}$, θ, q, and $\dot{\alpha}$. The work done by the aerodynamic forces can then be approximated by

$$\delta W = -\int_w (\mathrm{d}L\cos\alpha_0 + \mathrm{d}D\sin\alpha_0)y\delta\phi - \int_w (\mathrm{d}L\cos\alpha_0 + \mathrm{d}D\sin\alpha_0)x\delta\theta \tag{9}$$

This equation can be expanded in terms of variables p, β, $\dot{\beta}$, q, α, and $\dot{\alpha}$ and then integrated term by term. Even though the process is lengthy, it is straightforward. In general, the resulting integrands can be divided into two groups of odd and even terms. The odd terms are integrated to zero, and hence, the final result is the contribution of the even integrands only. Then by using $Q_i = \delta W_i/\delta\gamma_i$, the aerodynamic moments can be expressed as follows:

$$\begin{aligned}
\bar{Q}_1 &= \bar{c}_1\beta + \bar{c}_2 p + \bar{c}_3\dot{\beta} + \bar{c}_4\beta^3 + \bar{c}_5\beta^2 p + \bar{c}_6\beta^2\dot{\beta} + \bar{c}_7\beta p^2 \\
&\quad + \bar{c}_8\beta\dot{\beta}^2 + \bar{c}_9\dot{\beta}^3 + \bar{c}_{10}p^3 + \bar{c}_{11}\beta\alpha + \bar{c}_{12}\beta q + \bar{c}_{13}\beta\dot{\alpha} \\
&\quad + \bar{c}_{14}\dot{\beta}\alpha + \bar{c}_{15}\dot{\beta}q + \bar{c}_{16}\dot{\beta}\dot{\alpha} + \bar{c}_{17}p\alpha + \bar{c}_{18}pq + \bar{c}_{19}p\dot{\alpha} \\
&\quad + \bar{c}_{20}\beta\alpha^2 + \bar{c}_{21}\beta q^2 + \bar{c}_{22}\beta\dot{\alpha}^2 + \bar{c}_{23}\dot{\beta}\alpha^2 + \bar{c}_{24}\dot{\beta}q^2 \\
&\quad + \bar{c}_{25}\dot{\beta}\dot{\alpha}^2 + \bar{c}_{26}p\alpha^2 + \bar{c}_{27}pq^2 + \bar{c}_{28}p\dot{\alpha}^2 + \bar{c}_{29}\beta\alpha q \\
&\quad + \bar{c}_{30}p\alpha q + \bar{c}_{31}\dot{\beta}\alpha q + \bar{c}_{32}\beta\alpha\dot{\alpha} + \bar{c}_{33}p\alpha\dot{\alpha} + \bar{c}_{34}\dot{\beta}\alpha\dot{\alpha} \\
&\quad + \bar{c}_{35}\beta q\dot{\alpha} + \bar{c}_{36}pq\dot{\alpha} + \bar{c}_{37}\dot{\beta}q\dot{\alpha} + \bar{c}_{38}\beta\dot{\beta}p \\
\bar{Q}_2 &= \bar{d}_1\alpha + \bar{d}_2 q + \bar{d}_3\dot{\alpha} + \bar{d}_4\alpha^2 + \bar{d}_5\alpha q + \bar{d}_6\alpha\dot{\alpha} + \bar{d}_7 q^2 + \bar{d}_8 q\dot{\alpha} \\
&\quad + \bar{d}_9\dot{\alpha}^2 + \bar{d}_{10}\alpha^3 + \bar{d}_{11}\alpha^2 q + \bar{d}_{12}\alpha^2\dot{\alpha} + \bar{d}_{13}q^3 + \bar{d}_{14}q^2\alpha \\
&\quad + \bar{d}_{15}\alpha\dot{\alpha}^2 + \bar{d}_{16}q\dot{\alpha}^2 + \bar{d}_{17}q^2\dot{\alpha} + \bar{d}_{18}\dot{\alpha}^3 + \bar{d}_{19}\alpha q\dot{\alpha} + \bar{d}_{20}\alpha\beta^2 \\
&\quad + \bar{d}_{21}\alpha\beta p + \bar{d}_{22}\alpha\beta\dot{\beta} + \bar{d}_{23}\alpha p^2 + \bar{d}_{24}\alpha p\dot{\beta} + \bar{d}_{25}\alpha\dot{\beta}^2 + \bar{d}_{26}q\beta^2 \\
&\quad + \bar{d}_{27}q\beta p + \bar{d}_{28}q\beta\dot{\beta} + \bar{d}_{29}qp^2 + \bar{d}_{30}qp\dot{\beta} + \bar{d}_{31}q\dot{\beta}^2 + \bar{d}_{32}\dot{\alpha}\beta^2 \\
&\quad + \bar{d}_{33}\dot{\alpha}\beta p + \bar{d}_{34}\dot{\alpha}\beta\dot{\beta} + \bar{d}_{35}\dot{\alpha}p^2 + \bar{d}_{36}\dot{\alpha}p\dot{\beta} + \bar{d}_{37}\dot{\alpha}\dot{\beta}^2 \\
&\quad + \bar{d}_{38}\beta^2 + \bar{d}_{39}\beta p + \bar{d}_{40}p^2 + \bar{d}_{41}\beta\dot{\beta} + \bar{d}_{42}\dot{\beta}^2
\end{aligned} \tag{10}$$

where $\bar{Q}_1 \equiv Q_1/I_{xx}$ and $\bar{Q}_2 \equiv Q_2/I_{yy}$.

The next step is to express the equations of motion explicitly in $\ddot{\phi}$ and $\ddot{\theta}$ and in terms of ϕ and θ and their derivatives only. This can be done by using the following kinematic relations:

$$p = \dot{\phi}, \qquad \beta \approx \phi\sin\alpha_0, \qquad \dot{\beta} \approx \dot{\phi}\sin\alpha_0, \qquad q = \dot{\theta}$$
$$\alpha \equiv \theta, \qquad \dot{\alpha} \approx \dot{\theta} \tag{11}$$

The equations of motion of the aircraft then become (in matrix form)

$$\begin{bmatrix} 1 & n_1\phi \\ n_2\phi & 1 + (n_2/n_3)\phi^2 \end{bmatrix}\begin{pmatrix} \ddot{\phi} \\ \ddot{\theta} \end{pmatrix} = \begin{pmatrix} \hat{f}_1 \\ \hat{f}_2 \end{pmatrix} \tag{12}$$

where $n_1 \equiv I_{xz}/I_{xx}$, $n_2 \equiv I_{xz}/I_{yy}$, $n_3 \equiv I_{xz}/I_{zz}$, and

$$\hat{f}_1(\phi,\dot{\phi},\theta,\dot{\theta}) = \bar{Q}_1 - n_1\dot{\phi}\dot{\theta} + (n_1/n_3)\phi\dot{\theta}^2$$
$$\hat{f}_2(\phi,\dot{\phi},\theta,\dot{\theta}) = \bar{Q}_2 - n_2\dot{\phi}^2 - 2(n_2/n_3)\phi\dot{\phi}\dot{\theta} \tag{13}$$

By the inverse operation, we get

$$\begin{pmatrix} \ddot{\phi} \\ \ddot{\theta} \end{pmatrix} = \frac{1}{1 + (n_2/n_3 - n_1 n_2)\phi^2}\begin{bmatrix} 1 + \dfrac{n_2}{n_3}\phi^2 & -n_1\phi \\ -n_2\phi & 1 \end{bmatrix}\begin{pmatrix} \hat{f}_1 \\ \hat{f}_2 \end{pmatrix} \tag{14}$$

Because we are only interested in small values of ϕ, we approximate

$$1\Big/\left[1 + (n_2/n_3 - n_1 n_2)\phi^2\right] \approx 1 - (n_2/n_3 - n_1 n_2)\phi^2 \tag{15}$$

By substituting $\hat{f}_1$ and $\hat{f}_2$ from Eq. (13) into the preceding equations and retaining only terms up to third order, we get

$$\begin{aligned}
\ddot{\phi} + \omega^2\phi &= \tilde{\mu}\dot{\phi} + \tilde{c}_1\phi^3 + \tilde{c}_2\phi^2\dot{\phi} + \tilde{c}_3\phi\dot{\phi}^2 + \tilde{c}_4\dot{\phi}^3 + \tilde{c}_5\phi\theta \\
&\quad + \tilde{c}_6\phi\dot{\theta} + \tilde{c}_7\dot{\phi}\theta + \tilde{c}_8\dot{\phi}\dot{\theta} + \tilde{c}_9\phi\theta^2 + \tilde{c}_{10}\phi\dot{\theta}^2 \\
&\quad + \tilde{c}_{11}\dot{\phi}\theta^2 + \tilde{c}_{12}\dot{\phi}\dot{\theta}^2 + \tilde{c}_{13}\phi\theta\dot{\theta} + \tilde{c}_{14}\dot{\phi}\theta\dot{\theta} \\
\ddot{\theta} + \Omega^2\theta &= \tilde{\nu}\dot{\theta} + d_1\theta^2 + \tilde{d}_2\theta\dot{\theta} + \tilde{d}_3\dot{\theta}^2 + \tilde{d}_4\theta^3 + \tilde{d}_5\theta^2\dot{\theta} + \tilde{d}_6\theta\dot{\theta}^2 \\
&\quad + \tilde{d}_7\dot{\theta}^3 + \tilde{d}_8\theta\phi^2 + \tilde{d}_9\theta\phi\dot{\phi} + \tilde{d}_{10}\theta\dot{\phi}^2 + \tilde{d}_{11}\dot{\theta}\phi^2 \\
&\quad + \tilde{d}_{12}\dot{\theta}\phi\dot{\phi} + \tilde{d}_{13}\dot{\theta}\dot{\phi}^2 + \tilde{d}_{14}\phi^2 + \tilde{d}_{15}\phi\dot{\phi} + \tilde{d}_{16}\dot{\phi}^2
\end{aligned} \tag{16}$$

The relations between the coefficients in Eqs. (16) and (10) are given in Appendix A. Dynamic analysis in the subsequent sections is based on the preceding equations.

III. Motion Analysis

The MTS method[14,15] is first used to reduce the equations of motion into a set of first-order equations for the amplitude and phase of the dynamics. Center manifold reduction techniques along with the bifurcation theory are then applied to obtain an approximate solution and to assess the properties of the solution. Steady-state and transient motion analysis are both performed, and the results are compared with numerical solution.

A. MTS Analysis

The MTS concept described here is based on the development of Ramnath and Sandri[14] and Ramnath et al.[15] The MTS approach relies on the concept of extension. The fundamental idea of the concept of extension is to enlarge the domain of the independent variable to a space of higher dimension. Because our main interest is on dynamic systems, we will think of time as our independent variable. The independent variable, time, is extended to a set of new independent timelike variables, which are called time scales. Each time scale captures a certain behavior of the system. For example, the fast time scale captures only the fast behavior of the system. The extension of time t is symbolized as follows:

$$t \longrightarrow \{\tau_0, \tau_1, \ldots, \tau_n\} \tag{17}$$

where $\tau_0, \tau_1, \ldots, \tau_n$ are the time scales, which are normally functions of t and the small parameter ϵ, that is,

$$\tau_i = t_i(t,\epsilon), \qquad |\epsilon| \ll 1 \tag{18}$$

How τ_i relates to t determines the nature of the time scale. The relation of τ_i to ϵ in this case determines whether the time scale is fast or slow. Figure 2 shows a schematic of the concept.

With ordinary differential equation, the dependent variable $y(t,\epsilon)$ is also extended as

$$y(t,\epsilon) \longrightarrow Y(\tau_0, \tau_1, \ldots, \tau_n; \epsilon) \tag{19}$$

In applications, an ordinary differential equation will become a partial differential equation. This is not a limitation, however, because

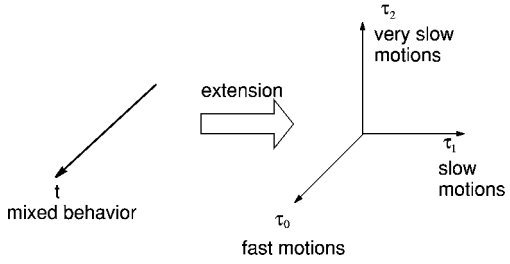

Fig. 2 Concept of extension.

the resulting partial differential equation is usually simpler than the initial ordinary differential equation.

Substitution of Eq. (18) into the extended function Y is called a restriction of Y:

$$Y[\tau_0(t,\epsilon), \tau_1(t,\epsilon), \ldots, \tau_n(t,\epsilon); \epsilon] = y(t,\epsilon) \tag{20}$$

We now focus on the small motions of the aircraft about its equilibrium conditions near wing rock situation. In such situations, for most aircraft θ and $\dot{\theta}$ are much smaller in magnitude than ϕ and $\dot{\phi}$. Observation of wing rock data for several aircraft confirms that the longitudinal oscillations are of much smaller amplitudes than the corresponding lateral oscillations.[9] Mathematically, we express this as $\mathcal{O}(|\boldsymbol{x}_2|) = \mathcal{O}(|\boldsymbol{x}_1|^2)$, where $\boldsymbol{x}_1^T = \{\phi \;\; \dot{\phi}\}$ and $\boldsymbol{x}_2^T = \{\theta \;\; \dot{\theta}\}$. Because of the small motion assumption, in the ϕ equation, we have

$$\lim_{x_1 \to 0} \frac{|f_1(\boldsymbol{x})|}{|\boldsymbol{x}_1|} = 0 \tag{21}$$

where $\boldsymbol{x} = \{\boldsymbol{x}_1^T \; \boldsymbol{x}_2^T\}^T$ and $f_1(\boldsymbol{x})$ contains all of the nonlinear terms in the ϕ equation. Similarly, for the θ equation, we have

$$\lim_{x_2 \to 0} \frac{|f_2(\boldsymbol{x})|}{|\boldsymbol{x}_2|} = 0 \tag{22}$$

where $f_2(\boldsymbol{x})$ contains all of the nonlinear terms in the θ equation, except for the nonlinear terms of the form ϕ, $\phi\dot{\phi}$, and $\dot{\phi}^2$ because these terms will be of $\mathcal{O}(|\boldsymbol{x}_2|)$ from the preceding discussion in this paragraph. As in the single-degree-of-freedom case and as we shall see later in the analysis, the roll damping parameter $\tilde{\mu}$ plays an important role in the wing rock dynamics. In the current case, this parameter is equivalent to the dynamic roll damping derivative, $L_{p_0} + L_{\dot{\beta}_0} \sin\alpha_0$. Note that the derivatives with subscript 0 indicate the derivatives that are usually found in the linear treatment of aircraft dynamics. Wing rock motion is normally caused by the loss of such damping. Because the analysis is focused on the aircraft motion in the vicinity of wing rock, this damping term is assumed to be small. Without loss of generality, the pitch damping parameter $\tilde{\nu}$ is also assumed to be small. Relaxation of this assumption does not affect the final results. Based on the preceding discussion and experience with numerical solutions of the problems, the following parameterization in terms of a small parameter ϵ is found to be constructive:

$$\begin{aligned} \ddot{\phi} + \omega^2\phi &= \epsilon[\mu\dot{\phi} + f_1(\phi, \dot{\phi}, \theta, \dot{\theta})] \\ \ddot{\theta} + \Omega^2\theta &= g(\phi, \dot{\phi}) + \epsilon[\nu\dot{\theta} + f_2(\phi, \dot{\phi}, \theta, \dot{\theta})] \end{aligned} \tag{23}$$

where $0 < \epsilon \ll 1$ and

$$\begin{aligned} g(\phi,\dot{\phi}) &= d_{14}\phi^2 + d_{15}\phi\dot{\phi} + d_{16}\dot{\phi}^2 \\ f_1(\phi,\dot{\phi},\theta,\dot{\theta}) &= c_1\phi^3 + c_2\phi^2\dot{\phi} + c_3\phi\dot{\phi}^2 + c_4\dot{\phi}^3 + c_5\phi\theta \\ &\quad + c_6\phi\dot{\theta} + c_7\dot{\phi}\theta + c_8\dot{\phi}\dot{\theta} + c_9\phi\theta^2 + c_{10}\phi\dot{\theta}^2 \\ &\quad + c_{11}\dot{\phi}\theta^2 + c_{12}\dot{\phi}\dot{\theta}^2 + c_{13}\phi\theta\dot{\theta} + c_{14}\dot{\phi}\theta\dot{\theta} \\ f_2(\phi,\dot{\phi},\theta,\dot{\theta}) &= d_1\theta^2 + d_2\theta\dot{\theta} + d_3\dot{\theta}^2 + d_4\theta^3 \\ &\quad + d_5\theta^2\dot{\theta} + d_6\theta\dot{\theta}^2 + d_7\dot{\theta}^3 + d_8\theta\phi^2 + d_9\theta\phi\dot{\phi} \\ &\quad + d_{10}\theta\dot{\phi}^2 + d_{11}\dot{\theta}\phi^2 + d_{12}\dot{\theta}\phi\dot{\phi} + d_{13}\dot{\theta}\dot{\phi}^2 \end{aligned} \tag{24}$$

The MTS method is now invoked. The independent variable t is extended into two time scales as follows:

$$t \to \{\tau_0, \tau_1\}, \qquad \tau_0 = t, \qquad \tau_1 = \epsilon t \tag{25}$$

In this case, τ_0 is the fast time scale, whereas τ_1 is the slow one. The dependent variables are also extended as

$$\begin{aligned} \phi(t) &\to \phi_0(\tau_0,\tau_1) + \epsilon\phi_1(\tau_0,\tau_1) + \cdots \\ \theta(t) &\to \theta_0(\tau_0,\tau_1) + \epsilon\theta_1(\tau_0,\tau_1) + \cdots \end{aligned} \tag{26}$$

The extended variables are then substituted into Eq. (23) and grouped according to the order of ϵ. Order by order analysis can then be performed by equating each group to zero.

Equations of leading order are given by

$$\frac{\partial^2\phi_0}{\partial\tau_0^2} + \omega^2\phi_0 = 0, \qquad \frac{\partial^2\theta_0}{\partial\tau_0^2} + \omega^2\theta_0 = g(\phi_0, \dot{\phi}_0) \tag{27}$$

The solution for the first equation is

$$\phi_0 = A_1(\tau_1)\sin\Psi_1, \qquad \Psi_1 \equiv \omega\tau_0 + B_1(\tau_1) \tag{28}$$

Then by substituting Eq. (28) into the second equation in Eq. (27), we get

$$\theta_0 = A_2(\tau_1)\sin\Psi_2 + m_0A_1^2 + m_1A_1^2\cos 2\Psi_1 + m_2A_1^2\sin 2\Psi_1 \tag{29}$$

where

$$\begin{aligned} \Psi_2 &\equiv \Omega\tau_0 + B_2(\tau_1), & m_0 &= \frac{d_{14} + d_{16}\omega^2}{2\Omega^2} \\ m_1 &= \frac{-d_{14} + d_{16}\omega^2}{2(\Omega^2 - 4\omega^2)}, & m_2 &= \frac{d_{15}\omega}{2(\Omega^2 - 4\omega^2)} \end{aligned} \tag{30}$$

Note that, from this solution, the pitch motion goes to a new equilibrium and contains oscillations with twice the frequency of the roll motion. The new equilibrium and the amplitude of the oscillations depend on the amplitude of the roll oscillations, the cross-coupling parameters, and on the dominant frequency of both roll and pitch oscillations. If the dominant pitch frequency is close to twice the roll frequency ($\Omega \approx 2\omega$), the denominator of m_1 and m_2 becomes close to zero and the approximate solution breaks down. This indicates an internal resonance situation, and clearly the approximate solutions obtained are not valid in such a situation. A different analysis has to be done to study such a situation. Because it occurs in only very special and limited cases, we will not discuss it further here.

The $\mathcal{O}(\epsilon)$ analysis results in the following equations:

$$\begin{aligned} \frac{\partial^2\phi_1}{\partial\tau_0^2} + \omega^2\phi_1 &= \left[-2\omega\frac{\mathrm{d}A_1}{\mathrm{d}\tau_1} + \mu\omega A_1 + \left(\frac{1}{4}c_2\omega + \frac{3}{4}c_4\omega^3\right.\right. \\ &\quad \left. + \frac{1}{2}m_2c_5 - m_1\omega c_6 + \frac{1}{2}c_7(2m_0 + m_1) + c_8m_2\omega^2\right)A_1^3 \\ &\quad \left. + \frac{1}{2}\omega\big(c_{11} + c_{12}\Omega^2\big)A_1A_2^2\right]\cos\Psi_1 + \left[2\omega A_1\frac{\mathrm{d}B_1}{\mathrm{d}\tau_1} + \frac{3}{4}c_1\right. \\ &\quad + \frac{1}{4}c_3\omega^2 + \frac{1}{2}c_5(2m_0 - m_1) - c_6m_2\omega + \frac{1}{2}\big(c_7m_2\omega \\ &\quad \left. - c_8m_1\omega^2\big)A_1^3 + \frac{1}{2}\big(c_9 + c_{10}\Omega^2\big)A_1A_2^2\right]\sin\Psi_1 + \cdots \\ \frac{\partial^2\theta_1}{\partial\tau_0^2} + \omega^2\theta_1 &= \frac{1}{2}\big(\mathrm{d}_1 + \mathrm{d}_3\Omega^2\big)A_2^3 + \frac{1}{2}d_{15}A_1\frac{\mathrm{d}A_1}{\mathrm{d}\tau_1} + d_{16}\omega A_1^2\frac{\mathrm{d}B_1}{\mathrm{d}\tau_1} \\ &\quad + \left[-2\Omega\frac{\mathrm{d}A_2}{\mathrm{d}\tau_1} + \nu\Omega A_2 + \frac{1}{4}\Omega\big(d_5 + 3d_7\Omega^2\big)A_2^3 + \Omega\left(d_2m_0\right.\right. \\ &\quad \left. \left. + \frac{1}{2}d_{11} + \frac{1}{2}d_{13}\omega^2\right)A_1^2A_2\right]\cos\Psi_2 + \left[2\Omega A_2\frac{\mathrm{d}B_2}{\mathrm{d}\tau_1} + \frac{1}{4}\big(3d_4\right. \\ &\quad \left. + d_6\Omega^2\big)A_2^3 + \frac{1}{2}(4d_1m_0 + d_8 + d_{10})A_1^2A_2\right]\sin\Psi_2 + \cdots \end{aligned} \tag{31}$$

We concentrate on the case where there is no internal resonance, that is,

$$l_1\Psi_1 \neq l_2\Psi_2 \tag{32}$$

where l_i are arbitrary integers. In this case, we see from Eq. (31) that the coefficients of the first harmonic terms must be set to zero so that no secular terms appear in the solution. By doing so, we get the following set of first-order equations for the amplitude and phase:

$$\frac{dA_1}{d\tau_1} = \frac{1}{2}\mu A_1 + p_1 A_1^3 + p_2 A_1 A_2^2$$

$$\frac{dA_2}{d\tau_1} = \frac{1}{2}\nu A_2 + q_1 A_2^3 + q_2 A_1^2 A_2$$

$$\frac{dB_1}{d\tau_1} = p_3 A_1^2 + p_4 A_2^2, \qquad \frac{dB_2}{d\tau_1} = q_3 A_1^2 + q_4 A_2^2 \tag{33}$$

where

$$p_1 = \tfrac{1}{8}\big[c_2 + 3c_4\omega^2 + (2/\omega)m_2c_5 - 4m_1c_6 + c_7(4m_0 + 2m_1) + 4c_8m_2\omega\big]$$

$$p_2 = \tfrac{1}{4}\big(c_{11} + c_{12}\Omega^2\big)$$

$$p_3 = -(1/8\omega)\big[3(c_1 + c_3)\omega^2 + c_5(4m_0 - 2m_1) - 4c_6m_2\omega + 2c_7m_2\omega - 4c_8m_1\omega^2\big]$$

$$p_4 = -(1/4\omega)\big[c_9 - n_1d_1 + c_{10}\Omega^2\big], \qquad q_1 = \tfrac{1}{8}\big(d_5 + 3d_7\Omega^2\big)$$

$$q_2 = \tfrac{1}{4}\big[2d_2m_0 + d_{11} + d_{13}\omega^2\big]$$

$$q_3 = -(1/4\Omega)[4d_1m_0 + d_8 + d_{10}]$$

$$q_4 = (1/8\Omega)\big(3d_4 + d_6\Omega^2\big) \tag{34}$$

Note that the first two equations in Eq. (33) are the amplitude equations, whereas the other two are the phase equations. The amplitude equations determine the amplitude history of the motion, whether the amplitudes of the motion decay or increase, hence, the stability of the motion. The phase equations give corrections to the frequency of the solution.

B. Center Manifold Reduction and Bifurcation Analysis

In this section, our focus is on the amplitude equations. Because the amplitude equations are coupled, we utilize the center manifold reduction technique to reduce the dimension of the system equations. The technique is based on the idea that the dynamics of the system are approached asymptotically by the dynamics on the center manifold. The main advantage of the technique is that the dynamic properties of the system can be obtained by examining the center manifold equations, which are generally of lower dimension than the complete system equations.

The center manifold of an equilibrium point is an invariant manifold that contains the equilibrium point and is tangent to the center eigenspace of the linearized system. In this case, the amplitude equations are of the following form:

$$\dot{\boldsymbol{x}} = \boldsymbol{A}\boldsymbol{x} + \boldsymbol{p}(\boldsymbol{x}, \boldsymbol{y}), \qquad \dot{\boldsymbol{y}} = \boldsymbol{B}\boldsymbol{y} + \boldsymbol{q}(\boldsymbol{x}, \boldsymbol{y}) \tag{35}$$

where $\boldsymbol{x} \in \boldsymbol{R}^l$, $\boldsymbol{y} \in \boldsymbol{R}^m$, and $\boldsymbol{A}$ and $\boldsymbol{B}$ are constant matrices such that $\Re(\lambda_i[\boldsymbol{A}]) = 0$, $i = 1, \ldots, l$, and $\Re(\lambda_i[\boldsymbol{B}]) < 0$, $i = 1, \ldots, m$. The functions $\boldsymbol{p}$ and $\boldsymbol{q}$ along with their Jacobians vanish at the origin, which is the equilibrium point of interest. In other words, $\boldsymbol{p}(\boldsymbol{0}, \boldsymbol{0}) = \boldsymbol{q}(\boldsymbol{0}, \boldsymbol{0}) = \boldsymbol{0}$ and $\nabla_p(\boldsymbol{0}, \boldsymbol{0}) = \nabla_q(\boldsymbol{0}, \boldsymbol{0}) = \boldsymbol{0}$. The linearized equation around the origin has two obvious eigenspaces, namely, $\boldsymbol{x} = \boldsymbol{0}$ and $\boldsymbol{y} = \boldsymbol{0}$, which represent stable and center eigenspaces, respectively. It is a well-known result that the system (35) possesses a local center manifold $\boldsymbol{y} = \boldsymbol{h}(\boldsymbol{x})$ for $|\boldsymbol{x}| < \delta$, $0 < \delta \ll 1$, where $\boldsymbol{h}(\boldsymbol{0}) = \nabla_h(\boldsymbol{0}) = \boldsymbol{0}$ (Refs. 16 and 17). The flow on the center manifold is then governed by the l-dimensional system:

$$\dot{\boldsymbol{z}} = \boldsymbol{A}\boldsymbol{z} + \boldsymbol{p}[\boldsymbol{z}, \boldsymbol{h}(\boldsymbol{z})] \tag{36}$$

Equation (36) contains all of the necessary information to determine the asymptotic behavior of the solutions of Eq. (35), as stated in the following theorem.[17]

Theorem A: The zero solution of Eq. (36) has the same stability property as the zero solution of Eq. (35).

Theorem B: Suppose the zero solution of Eq. (36) is stable. Let $[\boldsymbol{x}(t), \boldsymbol{y}(t)]$ be a solution of Eq. (35) with $[\boldsymbol{x}(0), \boldsymbol{y}(0)]$ sufficiently small. Then there exists a solution $\boldsymbol{z}(t)$ of Eq. (36) such that as $t \to \infty$

$$\boldsymbol{x}(t) = \boldsymbol{z}(t) + \mathcal{O}[\exp(-\gamma t)], \qquad \boldsymbol{y}(t) = \boldsymbol{h}[\boldsymbol{z}(t)] + \mathcal{O}[\exp(-\gamma t)] \tag{37}$$

where $\gamma > 0$ is a constant depending only on $\boldsymbol{B}$.

This result enables one to deal only with an l-dimensional equation, which is the dimension of the center manifold, to obtain the asymptotic behavior of the $(l + m)$-dimensional system.

In current problem, we consider the case where μ is small but not equal to zero. To put it into the center manifold framework, μ is considered as a trivial dependent variable in the formulation, as follows:

$$\frac{dA_1}{d\tau_1} = \frac{1}{2}\mu A_1 + p_1 A_1^3 + p_2 A_1 A_2^2$$

$$\frac{dA_2}{d\tau_1} = \frac{1}{2}\nu A_2 + q_1 A_2^3 + q_2 A_1^2 A_2, \qquad \frac{d\mu}{d\tau_1} = 0 \tag{38}$$

Note that in this formulation, the term $\frac{1}{2}\mu A_1$ is considered nonlinear. The equilibrium point of interest is the origin $(A_1, A_2, \mu) = (0, 0, 0)$. The linearization of the system (38) around the origin has eigenvalues 0, ν, and 0. By the assumption $\nu < 0$, the A_2 axis is a stable manifold. We will find a center manifold

$$A_2 = h(A_1, \mu) \tag{39}$$

that satisfies $h(0, 0) = (dh/dA_1)(0, 0) = (dh/d\mu)(0, 0) = 0$. Note that to satisfy this requirement $h = \mathcal{O}[(|A_1| + |\mu|)^n]$, $n > 1$. By differentiating Eq. (39) with respect to τ_1, we get

$$\frac{dA_2}{d\tau_1} = \frac{dh}{dA_1}\frac{dA_1}{d\tau_1} + \frac{dh}{d\mu}\frac{d\mu}{d\tau_1} \tag{40}$$

Then, by substituting $dA_1/d\tau_1$, $dA_2/d\tau_1$, and $d\mu/d\tau_1$ from Eq. (38) into Eq. (40), we obtain

$$\frac{dh}{dA_1} = \frac{\frac{1}{2}\nu h + q_1 h^3 + q_2 A_1^2 h}{\frac{1}{2}\mu A_1 + p_1 A_1^3 + p_2 A_1 h^2} \tag{41}$$

Because solving this equation is very difficult, we simplify it by remembering that $h = \mathcal{O}[(|A_1| + |\mu|)^n]$, $n > 1$, and neglecting terms in the numerator and denominator of $\mathcal{O}[(|A_1| + |\mu|)^k]$, $k > 3$. Doing so, we get

$$\frac{dh}{dA_1} \approx \frac{\frac{1}{2}\nu h}{\frac{1}{2}\mu A_1 + p_1 A_1^3} \tag{42}$$

It can be shown that the solution of the simplified equation is

$$h(A_1, \mu) = C\left(\frac{A_1^2}{\frac{1}{2}\mu + p_1 A_1^2}\right)^{\frac{1}{2}(\nu/\mu)} \tag{43}$$

where C is a constant to be determined from the condition $h(0, 0) = (dh/dA_1)(0, 0) = (dh/d\mu)(0, 0) = 0$. This condition can only be satisfied when

$$C = 0 \tag{44}$$

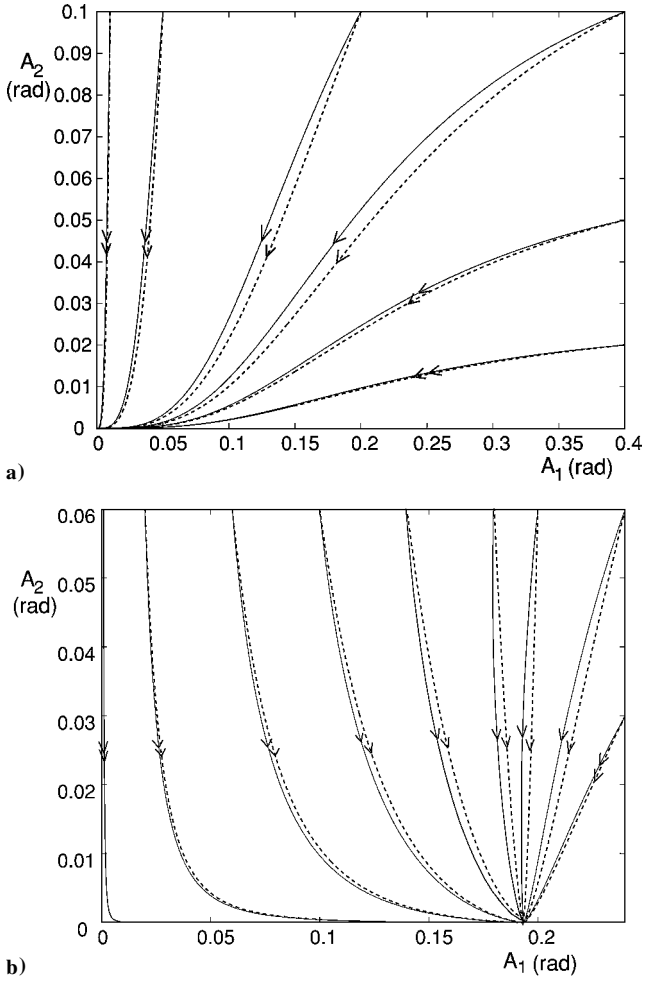

Fig. 3 Flow of the system for a) $\mu < 0$ and b) $\mu > 0$.

Therefore, the center manifold of the system is

$$A_2 = 0 \tag{45}$$

which is the A_1–μ plane.

The preceding result can also be deduced graphically. Figure 3 shows the flows of A_2 vs A_1 for $\mu < 0$ and for $\mu > 0$. In Fig. 3, the exact flows, shown using the solid curves, are compared to the approximate ones given by Eq. (43), represented by the dashed curves. We can see that the approximate solutions follow the exact solutions fairly well. It can also easily seen from Fig. 3 that the only solution that always satisfies $h(0, 0) = (\mathrm{d}h/\mathrm{d}A_1)(0, 0) = (\mathrm{d}h/\mathrm{d}\mu)(0, 0) = 0$ is $A_2 = 0$. It is clear then that $A_2 = 0$, that is, the A_1–μ plane, is the center manifold of the system.

The reduced system is then given by

$$\frac{\mathrm{d}A_1}{\mathrm{d}\tau_1} = \frac{1}{2}\mu A_1 + p_1 A_1^3, \qquad \frac{\mathrm{d}\mu}{\mathrm{d}\tau_1} = 0 \tag{46}$$

The equilibria of this system consist of the μ axis and the parabola $\mu = -2p_1 A_1^2$. Because $\mathrm{d}\mu/\mathrm{d}\tau_1 = 0$, the planes $\mu = \text{const}$ are invariant. In a plane $\mu = \text{const} \neq 0$, all of the equilibria are of hyperbolic type, and so their local stability properties can be assessed by looking at the eigenvalues of the linearized systems around the equilibria. The linearized system around the equilibria at μ axis for $\mu = \text{const} \neq 0$ is

$$\begin{Bmatrix} \dfrac{\mathrm{d}A_1}{\mathrm{d}\tau_1} \\ \dfrac{\mathrm{d}A_2}{\mathrm{d}\tau_1} \end{Bmatrix} = \begin{bmatrix} \dfrac{1}{2}\mu & 0 \\ 0 & \dfrac{1}{2}\nu \end{bmatrix} \begin{Bmatrix} A_1 \\ A_2 \end{Bmatrix} \tag{47}$$

The eigenvalues of the system are $\frac{1}{2}\mu$ and $\frac{1}{2}\nu$. Because ν is assumed to be negative, then the equilibria at μ axis is asymptotically stable if $\mu < 0$ and unstable if $\mu > 0$. Similarly, the linearized system around the equilibria $\mu = -2p_1 A_1^2$ for $\mu = \text{const} \neq 0$ is given by

$$\begin{Bmatrix} \dfrac{\mathrm{d}A_1}{\mathrm{d}\tau_1} \\ \dfrac{\mathrm{d}A_2}{\mathrm{d}\tau_1} \end{Bmatrix} = \begin{bmatrix} -\dfrac{1}{2}\mu & 0 \\ 0 & \dfrac{1}{2}\nu \end{bmatrix} \begin{Bmatrix} A_1 \\ A_2 \end{Bmatrix} \tag{48}$$

Here, the eigenvalues of the system are $-\frac{1}{2}\mu$ and $\frac{1}{2}\nu$. Hence, the equilibria at $\mu = -2p_1 A_1^2$ are asymptotically stable for $\mu > 0$ and unstable if $\mu < 0$.

At exactly $\mu = 0$, the reduced system becomes

$$\frac{\mathrm{d}A_1}{\mathrm{d}\tau_1} = p_1 A_1^3 \tag{49}$$

The stability properties of Eq. (49) can be studied without finding the exact solution. Note that $\mathrm{d}A_1/\mathrm{d}\tau_1$ determines the slope of the $A_1(\tau_1)$. If $p_1 > 0$, then $\mathrm{d}A_1/\mathrm{d}\tau_1 > 0$ for all τ_1, and $A_1(\tau_1)$ increases monotonically with τ_1. In this case, the system is unstable. On the other hand, if $p_1 < 0$, then $\mathrm{d}A_1/\mathrm{d}\tau_1 < 0$ for all τ_1, which means that $A_1(\tau_1)$ decreases monotonically with τ_1. This implies that the system is stable for $p_1 < 0$. For $p_1 = 0$, the stability of the system can only be determined by looking at higher-order terms.

The preceding discussion shows that the properties of the solution of the system change as μ varies from negative to positive. It is easy to see that the number of the equilibrium points changes across $\mu = 0$. Hence, $\mu = 0$ is the bifurcation point of the system. The bifurcation diagrams of this system for $p_1 > 0$ and $p_1 < 0$ are given in Fig. 4. These diagrams indicate that there is a finite amplitude oscillation of the limit-cycle-type appearing or disappearing in the system when μ is varied across $\mu = 0$. Hence, this is a Hopf-type bifurcation. When $p_1 > 0$, a subcritical Hopf bifurcation occurs, and there is no stable limit cycle in the system. When $p_1 < 0$, the Hopf bifurcation is supercritical, and a stable limit cycle appears for $\mu > 0$. Physically this means that a sustained wing rock motion can occur in the aircraft system. In this situation, $\mu = 0$ indicates the onset of wing rock.

An alternative argument can also be used to infer the presence of a Hopf bifurcation in the system by considering the variation of the eigenvalues of the linearized version of the equations of motion (23) as μ varies. In this case, there are two pairs of complex eigenvalues associated with the lateral and the longitudinal modes. Initially when $\mu < 0$, both pairs of the eigenvalues lie to the left of the imaginary axis, that is, in the stable region. As μ varies, the location of the eigenvalues changes. Exactly when $\mu = 0$, the pair of eigenvalues associated with the lateral mode lies on the imaginary axis. As μ increases further, these eigenvalues move to the right of the imaginary axis. The crossing of the imaginary axis occurs at a nonzero speed, and this condition gives rise to the occurence of

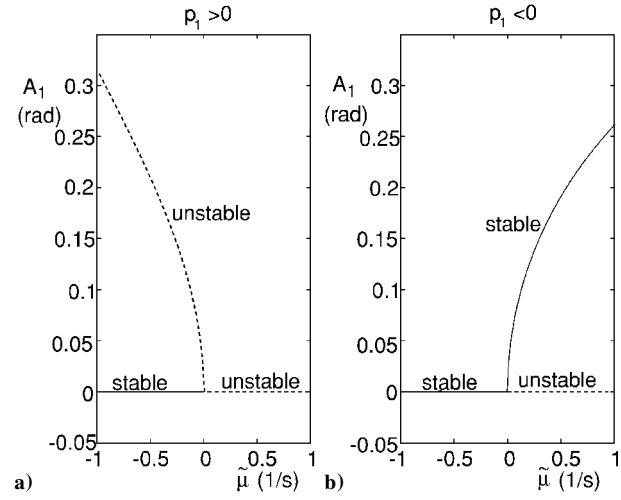

Fig. 4 Bifurcation diagrams for a) $p_1 > 0$ and b) $p_1 < 0$.

Hopf bifurcation. This type of analysis, however, does not tell us whether the bifurcation is subcritical or supercritical.

In the case where the stable limit cycle exists in the system, the amplitude of the limit cycle or, in other words, the amplitude of the wing rock motion, is given by

$$A_1 = \sqrt{-\mu/2p_1} \tag{50}$$

The preceding analysis can be interpreted as a steady-state analysis. This implies that after some transient, the amplitudes A_1 and A_2 eventually reach the steady-state values $A_1 = \sqrt{-(\mu/2p_1)}$ and $A_2 = 0$. The steady-state correction to the phase then can be calculated from the last two equations in Eq. (33), which yield

$$B_1 = -p_3(\mu/2p_1)\tau_1, \qquad B_2 = -q_3(\mu/2p_1)\tau_1 \tag{51}$$

C. Analytical Approximation of the Solution

We now develop a closed-form approximation of the system response, which includes the transient motion. We will solve the amplitude and phase equations (33). We will initially consider the amplitude differential equations. These equations are nonlinear and coupled, and the exact solutions can only be obtained by treating them together. We obtain an approximation to the exact solutions by applying Gronwall's lemma to the stable subset of the system, which is the second amplitude equation (recall the $\nu < 0$ assumption):

$$\frac{\mathrm{d}A_2}{\mathrm{d}\tau_1} = \frac{1}{2}\nu A_2 + g(A_1, A_2) \tag{52}$$

where $g(A_1, A_2) \equiv (q_1 A_2^2 + q_2 A_1^2)$.

Now suppose that one can find $0 < \delta \ll 1$ and $0 < \gamma < |\frac{1}{2}\nu|$ such that for $A_1, A_2 < \delta$, one has $|g(A_1, A_2)| \le \gamma A_2$. Because we only consider small amplitude motion, this condition can be easily satisfied. The integration of Eq. (52) yields

$$A_2(\tau_1) = \exp\left(\frac{1}{2}\nu\tau_1\right)A_{2_0} + \int_0^{\tau_1} \exp\left[\frac{1}{2}\nu(\tau_1 - s)\right] g(A_1, A_2)\,\mathrm{d}s \tag{53}$$

By the condition imposed on $|g(A_1, A_2)|$ and by multiplying both sides of the equation by $\exp(-\frac{1}{2}\nu\tau_1)$, we get

$$\exp\left(-\frac{1}{2}\nu\tau_1\right)|A_2(\tau_1)| \le A_{2_0} + \int_0^{\tau_1} \gamma \exp\left(-\frac{1}{2}s\right)|A_2|\,\mathrm{d}s \tag{54}$$

The statement of the Gronwall's lemma is given next. For proof, the reader may refer to Ref. 18.

Gronwall's lemma: If

$$f(t) \le K + \int_a^t f(s)g(s)\,\mathrm{d}s \tag{55}$$

for $a \le t \le b$, then $f(t)$ is bounded by

$$f(t) \le K \exp\left[\int_a^t g(s)\,\mathrm{d}s\right] \tag{56}$$

We see that Eq. (54) is in the form of Eq. (55) with $f(s) \equiv \exp(-\frac{1}{2}\nu s)|A_2(s)|$, $g(s) \equiv \gamma$, and $K \equiv A_{2_0}$. Therefore, it follows from the lemma that

$$\exp\left(-\tfrac{1}{2}\nu\tau_1\right)|A_2(\tau_1)| \le A_{2_0}\exp(\gamma\tau_1) \tag{57}$$

or

$$A_2(\tau_1) \le A_{2_0}\exp\left[\left(\tfrac{1}{2}\nu + \gamma\right)\tau_1\right] \tag{58}$$

This inequality provides the upper bound of the amplitude history of pitch motion θ.

When $g(A_1, A_2) = 0$, Eq. (52) becomes linear and the amplitude history is [from Eq. (53)]

$$\bar{A}_2(\tau_1) = A_{2_0}\exp\left(\tfrac{1}{2}\nu\tau_1\right) \tag{59}$$

where A_{2_0} is a constant determined from the initial conditions. The deviation of the actual A_2 history from Eq. (59) depends on the magnitude of $g(A_1, A_2)$, which is reflected in its upper bound γ. As a measure, we can examine the difference between the upper bound of A_2 and the linear solution $\bar{A}_2$ to get an idea of the magnitude of the deviation:

$$\Delta^u_{A_2} \equiv A_2 - \bar{A}_2 \le A_{2_0}\exp\left(\tfrac{1}{2}\nu\tau_1\right)[\exp(\gamma\tau_1) - 1] \tag{60}$$

This is equivalent to

$$\Delta^u_{A_2} \big/ \bar{A}_2 \le \exp(\gamma\tau_1) - 1 \tag{61}$$

This means that, for small γ, $\bar{A}_2$ is a good approximation to the actual A_2 history. Because we are only interested in small-amplitude motions and $|g(A_1, A_2)|$ is of the order of square of the amplitudes, then γ can be taken to be very small. Therefore, for our purposes we will use $\bar{A}_2$ as the approximation to the A_2 history.

The substitution of $\bar{A}_2$ into the A_1 differential equation in Eq. (38) yields

$$\frac{\mathrm{d}A_1}{\mathrm{d}\tau_1} = a(\tau_1)A_1 + p_1 A_1^3 \tag{62}$$

where

$$a(\tau_1) = \tfrac{1}{2}\mu + p_2 A_{2_0}^2 \exp(\nu\tau_1) \tag{63}$$

Equation (62) is a first-order nonlinear differential equation with a time-varying coefficient in $a(\tau_1)$, the solution of which can be shown to be (see Ref. 13 for the derivation)

$$A_1 = \frac{\exp\left[\int a(\tau_1)\,\mathrm{d}\tau_1\right]}{\sqrt{C_1 - 2p_1 \int \exp\left[2\int a(\tau_1)\,\mathrm{d}\tau_1\right]\mathrm{d}\tau_1}} \tag{64}$$

The constant C_1 in Eq. (64) is determined from the initial condition. The integral

$$\int \exp\left[2\int a(\tau_1)\,\mathrm{d}\tau_1\right]\mathrm{d}\tau_1$$

is not simple to obtain because $a(\tau_1)$ also contains an exponential term. Here we attempt to assess some of its properties without evaluating it.

From Eq. (63), we observe that the second term on the right-hand side is of $\mathcal{O}(A_{2_0}^2)$. Because we are only interested in small-amplitude motion, then the effect of this term is generally small. Moreover, because $\nu < 0$, this term goes to zero exponentially as τ_1 increases. When $\tau_1 = 0$, then

$$\int \exp\left[2\int a(\tau_1)\,\mathrm{d}\tau_1\right]\mathrm{d}\tau_1 = 0 \tag{65}$$

For large τ_1,

$$\int \exp\left[2\int a(\tau_1)\,\mathrm{d}\tau_1\right]\mathrm{d}\tau_1 \approx \frac{2}{\mu}\exp\left(\frac{\mu}{2}\tau_1\right) \tag{66}$$

and as $\tau_1 \to \infty$,

$$\begin{aligned} \exp[(\mu/2)\tau_1] &\to 0 \quad \text{for} \quad \mu < 0 \\ \exp[(\mu/2)\tau_1] &\to \infty \quad \text{for} \quad \mu > 0 \end{aligned} \tag{67}$$

The stability of motion for $\mu = 0$ is described by the center manifold analysis presented in Sec. III.B.

From the preceding discussion, if we let the initial condition for A_1 to be A_{1_0}, then we get C_1 in terms of A_{1_0} from Eq. (64) as follows:

$$A_{1_0}^2 = 1/C_1 \iff C_1 = 1\big/A_{1_0}^2 \tag{68}$$

Hence, in terms of A_{1_0},

$$A_1 = A_{1_0}\frac{\exp\left[\int a(\tau_1)\,\mathrm{d}\tau_1\right]}{\sqrt{1 - 2p_1 A_{1_0}^2 \int \exp\left[2\int a(\tau_1)\,\mathrm{d}\tau_1\right]\mathrm{d}\tau_1}} \tag{69}$$

The solutions for B_1 and B_2 then follow in a straightforward manner. From the preceding discussion, we can then obtain the steady-state

condition of the A_1 history. As $\tau_1 \to \infty$, the second term in the denominator is much greater in magnitude than 1, and, thus,

$$A_1 \to 0 \qquad \text{for} \qquad \mu < 0$$

$$A_1 \to \sqrt{-\frac{\exp(\mu\tau_1)}{2(p_1/\mu)\exp(\mu\tau_1)}} = \sqrt{-\frac{\mu}{2p_1}} \quad \text{for} \quad \mu > 0 \qquad (70)$$

This result is consistent with the result from steady-state center manifold analysis in Sec. III.B.

The result shows the importance of the parameters μ and p_1 on wing rock characteristics. The onset of wing rock is determined by μ, whereas its amplitude is determined by both μ and p_1. As mentioned, μ for this two-degrees-of-freedom problem is equivalent to dynamic roll damping derivative. Thus, the onset of wing rock in this case is the same as in the roll-only, single-degree-of-freedom case, which is a special case of the current problem.[4,7,13] Here p_1 is built up mainly by the aerodynamic nonlinearity. Notice from the definition of p_1 in Eq. (34) that its value is affected by some longitudinal parameters. Therefore, in general, the amplitude of two-degrees-of-freedom wing rock motion is not the same as the amplitude of the single-degree-of-freedom case.

IV. Comparison with Numerical Results

A generic fighter aircraft model is used to illustrate and validate our analytical representation of the dynamics of the aircraft motion in the vicinity of wing rock. The model involves nonlinearities in many aspects of aircraft aerodynamics, that is, nonlinear variation with angle of sideslip, rotation rate, and angle of attack.

The parameters of the aircraft and its aerodynamic model as used in the simulation are given in Appendix B. This model is valid only for angle-of-attack values in the range 20–40 deg, which is the range where transition to wing rock motion occurs. For this aircraft, the variation of the wing rock damping parameter μ and the parameter p_1 with the nominal angle of attack are given in Fig. 5.

A simulation of the aircraft response for nominal angle of attack of 32 deg is shown in Fig. 6. At this angle of attack, μ is positive and the wing rock motion is developed, as can be seen from Fig. 6. Note that, in Fig. 6, the analytical approximation obtained in the preceding section is compared to the solution as obtained using numerical integration. In this case, the analytical approximation is in excellent agreement with the numerical integration result. The amplitude and phase history are predicted very accurately by the analytical solution. Note also that, for pitch motion, the analytical approximation correctly predicts the existence of the new equilibrium and the sustained oscillation with twice the frequency of the roll motion.

To examine the accuracy of the prediction of the wing rock onset, a simulation of the aircraft responses slightly below and slightly above the onset point is performed. For the aircraft model, the wing rock onset is at $\alpha_0 = 27.34$ deg. Numerical and analytical simulation of the system response for $\alpha_0 = 27.2$ and 27.5 deg are given in Fig. 7. This example shows that our analytical development predicts the dynamics of the aircraft in the vicinity of wing rock very accurately, even though the aerodynamic model used in the example is quite complicated.

The present analysis subsumes most previous work, where only the effects of specific type of nonlinearity are considered. Clearly, we can examine the effect of a specific nonlinearity. Examples of this are given in Ref. 13. Some interesting facts from the examination of the effects of certain nonlinearity are mentioned here. As in the single-degree-of-freedom case, a cubic variation of rolling moment with sideslip, by itself, does not cause wing rock. Such a nonlinearity only causes a slight increase or decrease in the frequency of the aircraft oscillation. An effect that is not captured by a single-degree-of-freedom model is the dynamic cross-coupling aerodynamic derivatives. As is shown in Ref. 13, a relatively strong linear dependency of such derivatives with sideslip angle can give rise to wing rock. In such situations, energy transfer occurs between roll and pitch modes of the aircraft and may give rise to a more complex situation.

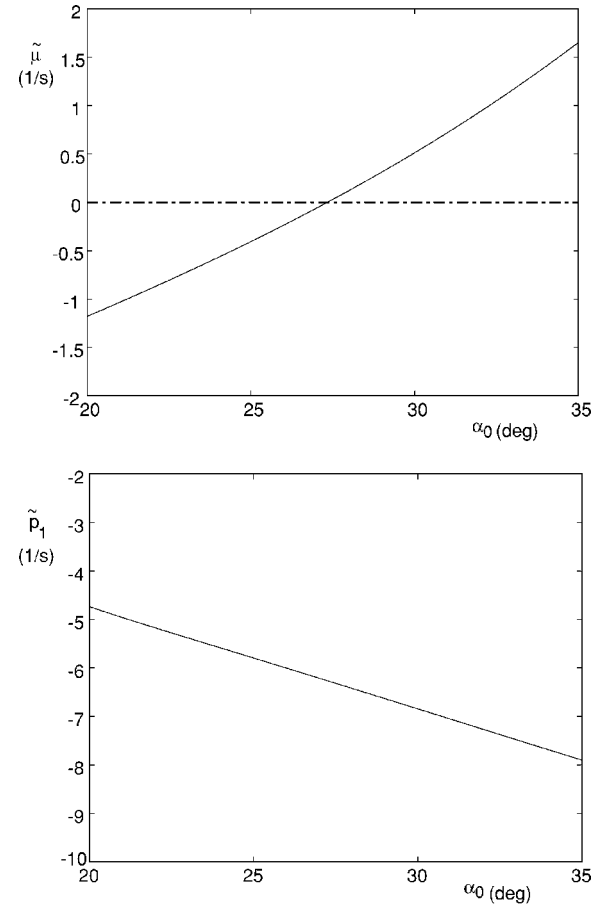

Fig. 5 Variation of $\tilde{\mu}$ and $\tilde{p}_1$ with α_0.

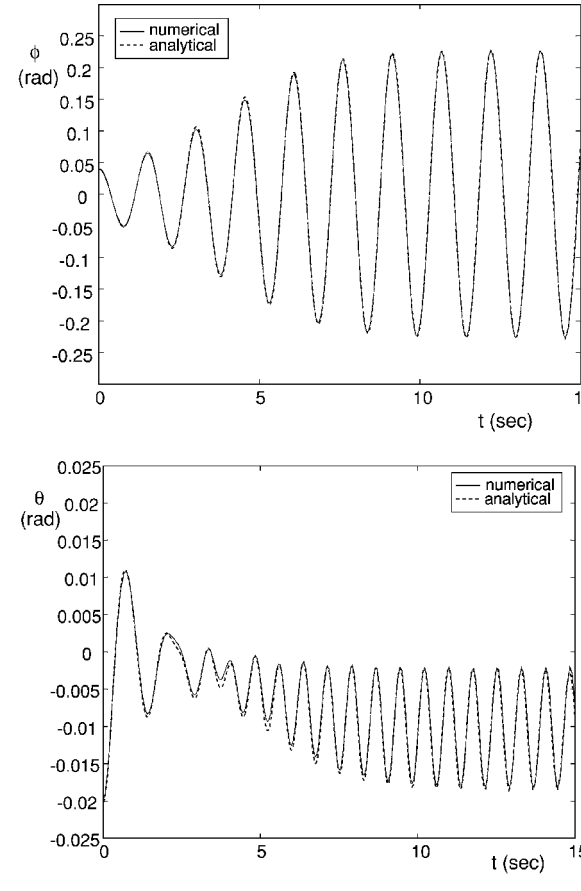

Fig. 6 Roll and pitch angle response at $\alpha_0 = 31$ deg and initial condition $(\phi_0, \theta_0) = (0.04, -0.02)$ rad.

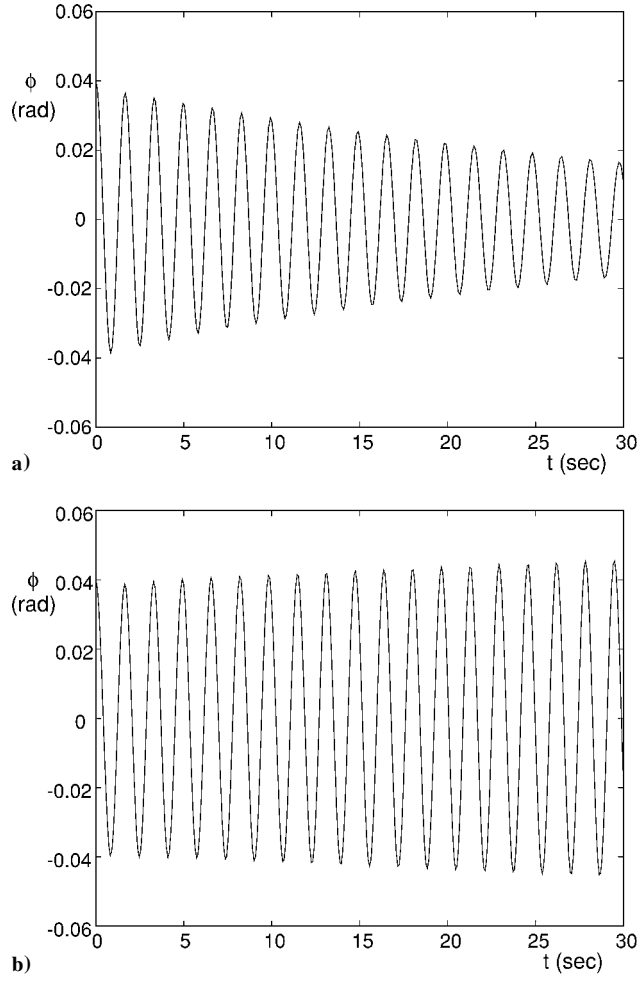

Fig. 7 Aircraft response for a) $\alpha_0 = 27.2$ deg and b) 27.5 deg.

V. Conclusions

Wing rock dynamics of an aircraft having two degrees of freedom in roll and pitch have been considered. The analysis technique using the MTS method, center manifold reduction principle, and bifurcation theory describes the system dynamics successfully leading to the solutions in closed parametric form. Compared to the result of the single-degree-of-freedom problem, the onset of wing rock is not affected by the additional degree of freedom in pitch. However, the amplitude of the resulting wing rock motion in the two-degrees-of-freedom case is generally different from the single-degree-of-freedom case because the effect of the longitudinal and coupling parameters. An interesting aspect of the dynamics that is not captured by the single-degree-of-freedom model is the steady-state pitch oscillation around a new equilibrium state with twice the frequency of the wing rock motion. All of these suggest that the simplified single-degree-of-freedom model has to be used with caution because it may not capture all of the important aspects of the system dynamics. As seen from our analysis, the longitudinal dynamics may appear to be not as significant as the lateral dynamics. However, as has been shown analytically, it has quite a significant effect on the wing rock properties in general.

Appendix A: Relations Between Coefficients of Eqs. (16) and (10)

Roll equation:

$$\omega^2 = -\bar{c}_1 \sin\alpha_0, \qquad \tilde{\mu} = \bar{c}_2 + \bar{c}_3 \sin\alpha_0$$

$$\tilde{c}_1 = (n_2/n_3 - n_1 n_2)\,\bar{c}_1 \sin\alpha_0 + \bar{c}_4 \sin^3\alpha_0 - n_1 \bar{d}_{38} \sin^2\alpha_0$$

$$\tilde{c}_2 = (n_2/n_3 - n_1 n_2)(\bar{c}_2 + \bar{c}_3 \sin\alpha_0) + \bar{c}_5 \sin^2\alpha_0 + \bar{c}_6 \sin^3\alpha_0 - n_1(\bar{d}_{39} + \bar{d}_{41} \sin\alpha_0) \sin\alpha_0$$

$$\tilde{c}_3 = \bar{c}_7 \sin\alpha_0 + \bar{c}_{38} \sin^2\alpha_0 + \bar{c}_8 \sin^3\alpha_0 - n_1\left(-n_2 + \bar{d}_{40} + \bar{d}_{42} \sin^2\alpha_0\right)$$

$$\tilde{c}_4 = \bar{c}_9 \sin^3\alpha_0 + \bar{c}_{10}, \qquad \tilde{c}_5 = \bar{c}_{11} \sin\alpha_0 - n_1 \bar{d}_1$$

$$\tilde{c}_6 = (\bar{c}_{12} + \bar{c}_{13}) \sin\alpha_0 - n_1(\bar{d}_2 + \bar{d}_3), \qquad \tilde{c}_7 = \bar{c}_{14} \sin\alpha_0 + \bar{c}_{17}$$

$$\tilde{c}_8 = -n_1 + (\bar{c}_{15} + \bar{c}_{16}) \sin\alpha_0 + \bar{c}_{18} + \bar{c}_{18}, \qquad \tilde{c}_9 = \bar{c}_{20} - n_1 \bar{d}_4$$

$$\tilde{c}_{10} = n_1/n_3 + (\bar{c}_{21} + \bar{c}_{22} + \bar{c}_{35}) \sin\alpha_0 - n_1(\bar{d}_7 + \bar{d}_8 + \bar{d}_9)$$

$$\tilde{c}_{11} = \bar{c}_{23} \sin\alpha_0 + \bar{c}_{26}$$

$$\tilde{c}_{12} = (\bar{c}_{24} + \bar{c}_{25} + \bar{c}_{37}) \sin\alpha_0 + \bar{c}_{27} + \bar{c}_{28} + \bar{c}_{36}$$

$$\tilde{c}_{13} = (\bar{c}_{29} + \bar{c}_{32}) \sin\alpha_0 - n_1(\bar{d}_5 + \bar{d}_6)$$

$$\tilde{c}_{14} = \bar{c}_{30} + \bar{c}_{33} + (\bar{c}_{31} + \bar{c}_{34}) \sin\alpha_0$$

Pitch equation:

$$\Omega^2 = -\bar{d}_1, \qquad \tilde{\nu} = (\bar{d}_2 + \bar{d}_3), \qquad \tilde{d}_1 = \bar{d}_4, \qquad \tilde{d}_2 = \bar{d}_5 + \bar{d}_6$$

$$\tilde{d}_3 = \bar{d}_7 + \bar{d}_8 + \bar{d}_9, \qquad \tilde{d}_4 = \bar{d}_{10}, \qquad \tilde{d}_5 = \bar{d}_{11} + \bar{d}_{12}$$

$$\tilde{d}_6 = \bar{d}_{14} + \bar{d}_{15} + \bar{d}_{19}, \qquad \tilde{d}_7 = \bar{d}_{13} + \bar{d}_{16} + \bar{d}_{17} + \bar{d}_{18}$$

$$\tilde{d}_8 = (-n_2/n_3 + n_1 n_3)\bar{d}_1 + \bar{d}_{20} \sin^2\alpha_0 - n_2 \bar{c}_{11} \sin\alpha_0$$

$$\tilde{d}_9 = (\bar{d}_{21} + \bar{d}_{22}) \sin\alpha_0 - n_2(\bar{c}_{14} \sin\alpha_0 + \bar{c}_{17})$$

$$\tilde{d}_{10} = \bar{d}_{23} + (\bar{d}_{24} + \bar{d}_{25} \sin\alpha_0) \sin\alpha_0$$

$$\tilde{d}_{11} = (-n_2/n_3 + n_1 n_2)(\bar{d}_2 + \bar{d}_3) + (\bar{d}_{26} + \bar{d}_{32}) \sin\alpha_0 - n_2(\bar{c}_{12} + \bar{c}_{13}) \sin\alpha_0$$

$$\tilde{d}_{12} = -2(n_2/n_3) + n_1 n_2 + (\bar{d}_{27} + \bar{d}_{33}) \sin\alpha_0 + (\bar{d}_{28} + \bar{d}_{34}) \sin^2\alpha_0 - n_2[(\bar{c}_{15} + \bar{c}_{16}) \sin\alpha_0 + \bar{c}_{18} + \bar{c}_{19}]$$

$$\tilde{d}_{13} = \bar{d}_{29} + \bar{d}_{35} + (\bar{d}_{30} + \bar{d}_{36}) \sin\alpha_0 + (\bar{d}_{31} + \bar{d}_{37}) \sin^2\alpha_0$$

$$\tilde{d}_{14} = \bar{d}_{38} \sin^2\alpha_0 - n_2 \bar{c}_1 \sin\alpha_0$$

$$\tilde{d}_{15} = (\bar{d}_{39} + \bar{d}_{41} \sin\alpha_0) \sin\alpha_0 - n_2(\bar{c}_2 + \bar{c}_3 \sin\alpha_0)$$

$$\tilde{d}_{16} = -n_2 + \bar{d}_{40} + \bar{d}_{42} \sin^2\alpha_0$$

Appendix B: Generic Fighter Aircraft Parameters for $20 \le \alpha_0 \le 40$ Degrees

$$I_{xx} = 36{,}610 \text{ kg m}^2, \qquad I_{yy} = 162{,}700 \text{ kg m}^2$$

$$I_{zz} = 183{,}000 \text{ kg m}^2, \qquad I_{xz} = 6780 \text{ kg m}^2$$

$$b = 12 \text{ m}, \qquad c = 4.8 \text{ m}, \qquad S = 164.6 \text{ m}^2$$

$$\rho = 1.225 \text{ kg/m}^3, \qquad V = 100 \text{ m/s}$$

$$C_l = \left(-0.295\alpha_0 + 0.1975\alpha_0^2\right)\beta + \left(-0.22 + 0.63\alpha_0 - 0.797\alpha_0^2 + 0.975\alpha_0^3\right)\frac{bp}{2V} + 0.4\beta^2\frac{bp}{2V} - 0.075\left(\frac{bp}{2V}\right)^3 - 1.42\beta\left(\frac{bp}{2V}\right)^2 - 0.011\dot{\beta} - 0.08\alpha\beta + 0.236\alpha^2\beta + 0.56\alpha\frac{bp}{2V} + 0.09\alpha^2\frac{bp}{2V} + 1.6\alpha\dot{\beta} - 6.1\alpha^2\dot{\beta} + 0.5\beta\frac{cq}{2V} + 30\alpha\beta\frac{cq}{2V}$$

$$C_m = -0.68\alpha - 2\frac{cq}{2V} - 0.75\alpha^2 - 3.75\alpha^3 + 0.7\left(\frac{cq}{2V}\right)^3$$
$$+ 0.58\alpha\frac{cq}{2V} + 3.564\alpha^2\frac{cq}{2V} + 0.4\beta\frac{cq}{2V} - 4.01\beta^2$$
$$+ 0.26\alpha\beta^2 + 0.1\beta\frac{bp}{2V} + 0.5\alpha\beta\frac{bp}{2V}$$

References

[1]Ericsson, L. E., "The Fluid Mechanics of Slender Wing Rock," *Journal of Aircraft*, Vol. 21, No. 5, 1984, pp. 322–328.

[2]Ericsson, L. E., "Analytic Prediction of the Maximum Amplitude of Slender Wing Rock," *Journal of Aircraft*, Vol. 26, No. 1, 1989, pp. 35–39.

[3]Nguyen, L. T., Yip, L., and Chambers, J. R., "Self-Induced Wing Rock of Slender Delta Wings," AIAA Paper 81-1883, 1981.

[4]Hsu, C., and Lan, C. E., "Theory of Wing Rock," *Journal of Aircraft*, Vol. 22, No. 10, 1985, pp. 920–924.

[5]Konstadinopoulos, P., Mook, D. T., and Nayfeh, A. H., "Subsonic Wing Rock of Slender Delta Wings," *Journal of Aircraft*, Vol. 22, No. 3, 1985, pp. 223–228.

[6]Elzebda, J. M., Nayfeh, A. H., and Mook, D. T., "Development of an Analytical Model of Wing Rock for Slender Delta Wings," *Journal of Aircraft*, Vol. 26, No. 8, 1989, pp. 737–743.

[7]Nayfeh, A. H., Elzebda, J. M., and Mook, D. T., "Analytical Study of the Subsonic Wing-Rock Phenomenon for Slender Delta Wings," *Journal of Aircraft*, Vol. 26, No. 9, 1989, pp. 805–809.

[8]Elzebda, J. M., Mook, D. T., and Nayfeh, A. H., "Influence of Pitching Motion on Subsonic Wing Rock of Slender Delta Wings," *Journal of Aircraft*, Vol. 26, No. 6, 1989, pp. 503–508.

[9]Johnston, D. E., "Identification of Key Maneuver-Limiting Factors in High Angle-of-Attack Flight," *Dynamic Stability Parameters*, CP-235, AGARD, 1978.

[10]Planeaux, J. B., and Barth, T. J., "High-Angle-of-Attack Dynamic Behavior of a Model High-Performance Fighter Aircraft," AIAA Paper 88-4368, 1988.

[11]Planeaux, J. B., Beck, J. A., and Baumann, D. D., "Bifurcation Analysis of a Model Fighter Aircraft with Control Augmentation," AIAA Paper 90-2836, 1990.

[12]Jahnke, C. J., "Application of Dynamical Systems Theory to Nonlinear Aircraft Dynamics," Ph.D. Dissertation, California Inst. of Technology, Pasadena, CA, Jan. 1990.

[13]Go, T. H., "Aircraft Wing Rock Dynamics and Control," Sc.D. Dissertation, Dept. of Aeronautics and Astronautics, Massachusetts Inst. of Technology, Cambridge, MA, Sept. 1999.

[14]Ramnath, R. V., and Sandri, G., "A Generalized Multiple Scales Approach to a Class of Linear Differential Equations," *Journal of Mathematical Analysis and Applications*, Vol. 28, Nov. 1969, pp. 339–364.

[15]Ramnath, R. V., Hedrick, J. K., and Paynter, H. M. (eds.), *Nonlinear Systems Analysis and Synthesis*, Vol. 2, Techniques and Applications, American Society of Mechanical Engineers, Fairfield, NJ, 1981, pp. 3–54.

[16]Guckenheimer, J., and Holmes, P., *Nonlinear Oscillations, Dynamical Systems, and Bifurcations of Vector Fields*, Springer-Verlag, New York, 1983.

[17]Carr, J., *Applications of Centre Manifold Theory*, Springer-Verlag, New York, 1981.

[18]Hale, J. K., and Kocak, H., *Dynamics and Bifurcations*, Springer-Verlag, New York, 1991.